Punicalagin induces senescent growth arrest in human papillary thyroid carcinoma BCPAP cells *via* NF-κB signaling pathway

Xian Cheng[a,1], Xin Yao[b,1], Shichen Xu[a,b], Jie Pan[b], Huixin Yu[a], Jiandong Bao[a,c], Haixia Guan[d], Rongrong Lu[b], Li Zhang[a,*]

[a] *Key Laboratory of Nuclear Medicine, Ministry of Health, Jiangsu Key Laboratory of Molecular Nuclear Medicine, Jiangsu Institute of Nuclear Medicine, Wuxi, Jiangsu, China*
[b] *School of Food Science and Technology, Jiangnan University, Wuxi, Jiangsu, China*
[c] *Department of Endocrinology, JiangYuan Hospital Affiliated to Jiangsu Institute of Nuclear Medicine. Wuxi, Jiangsu, China*
[d] *Department of Endocrinology & Metabolism and Institute of Endocrinology, the First Hospital of China Medical University, Shenyang, Liaoning, China*

ARTICLE INFO

ABSTRACT

Papillary thyroid carcinoma (PTC) is the most common endocrine carcinoma. Our previous study revealed that punicalagin (PUN), an active component from pomegranate, triggered autophagic cell death and DNA damage response (DDR) in papillary thyroid carcinoma BCPAP cells. But the detailed anti-cancer mechanisms of punicalagin against PTC still remained to be further explored. DDR activation is a proven cause of cellular senescence, which mediates anti-tumor processes under certain circumstances. In this study, we reported that punicalagin treatment generated a senescent phenotype of BCPAP cells characterized as altered morphology, increased cell granularity and senescence-associated β-galactosidase (SA-β-Gal) staining. Senescence induced by punicalagin treatment was further confirmed by cell cycle arrest and upregulation of cyclin-dependent kinase inhibitor p21. Meanwhile, the senescence-associated secretory phenotype (SASP) included high levels of inflammatory cytokines, principally IL-6 and IL-1β. Furthermore, punicalagin exposure caused the phosphorylation and subsequent degradation of IκBα as well as the nuclear translocation of p65, suggesting the activation of NF-κB signaling pathway. Inhibition of NF-κB by pyrrolidine dithiocarbamate (PDTC), a selective inhibitor of NF-κB, partially reversed the cellular senescent phenotype induced by punicalagin in BCPAP cells as evidenced by the decreased fraction of SA-β-Gal staining positive cells and blockage of SASP generation. These results collectively showed that punicalagin treatment induced senescent growth arrest and SASP *via* triggering NF-κB activation. These observations elucidated novel anti-cancer mechanisms of punicalagin and might provide new potential prospects for PTC therapy.

1. Introduction

Cellular senescence is typically characterized as an irreversible cell cycle arrest which can be triggered by various environmental and genetic factors, such as UV exposure, DNA damage and oncogenes [1]. The eternal abrogation of cell cycle brings a catastrophic attack to tissue renewal and cell homeostasis, which will result in a distinct senescence-like phenotype as indicated by enlarged morphology, SA-β-Gal staining and upregulation of cyclin dependent kinase inhibitors (CDKIs) [2]. Accumulating studies have highlighted the fact that cellular senescence could contribute to the anti-tumorigenic therapy [3]. A variety of anti-cancer agents have been reported to be able to induce senescence of different tumor cell lines. Senescent cells could secrete senescence-associated secretory phenotype (SASP) including pro-inflammatory cytokines and chemokines to further influence the surrounding environment [4]. The secreted SASP, especially some pro-inflammatory cytokines, which are tightly regulated by NF-κB pathway, can recruit immune cells to clear up the damaged cells and premalignant cells to prevent tumorigenesis [5]. Indeed, targeting cellular senescence has been reported to inhibit the progression of liver carcinoma [6], prostate tumorigenesis [7], thyroid cancer [8] and so on.

Thyroid cancer is the most common endocrine cancer with an increased incidence and mortality [9]. Papillary thyroid carcinoma (PTC) is the major type of thyroid cancer. Surgical thyroidectomy, hormone suppression and radiotherapy are conventional treatment methods for PTC therapy and patients usually have a good prognosis. However,

---

there is still a certain amount of patients, especially those harboring *BRAF* and *TERT* mutations, will more likely possess a recurrent or metastatic stage. Some of them will even develop into a kind of radioactive iodine-refractory differentiated thyroid cancer (RAI-*R*-DTC) [10]. The strategy for treating these aggressive thyroid cancer patients remained an arduous task. Multi-targeted inhibitors including sorafenib and levatinib have been approved by FDA for the thyroid cancer molecular targeting therapy [11]. Nevertheless, developing novel therapy strategies or searching for new drugs is still an urgent for the therapy of aggressive and RAI-*R*-DTC patients.

Punicalagin (PUN) acts as a natural anti-cancer agent against various malignant tumors including colon and glioma cancer [12]. Our previous studies showed that punicalagin treatment could not only trigger autophagic cell death [13] but also induce DNA damage response (DDR) of thyroid cancer cells after 24 h incubation [14]. However, the long-term effect of punicalagin on thyroid cancer cells remains to be further defined. Considering both autophagy and DDR are closely related with cellular senescence [15], it is reminiscent of the possibility that cellular senescence might also be involved in the growth inhibition effects of punicalagin on thyroid cancer cells.

In the present study, we addressed that punicalagin inhibited the proliferation of thyroid cancer BCPAP cells by inducing irreversible senescent cell cycle arrest. Our study illustrated a new anti-cancer mechanism of punicalagin and provided a promising anti-cancer target for PTC therapy.

2. Materials and methods

2.1. Chemicals, reagents and antibodies

Punicalagin (PUN, HPLC $\geq$98%) was purchased from klamar-reagent (Shanghai puzhen Biotechnology Co., Ltd). Newborn calf serum (NCS) was purchased from Zhejiang Tianhang Biological Technology Co., Ltd. Methyl thiazolyl tetrazolium (MTT) and dimethyl sulfoxide (DMSO) were purchased from Sangon (Shanghai, China). SA-β-Gal staining kit, Nuclear Protein and Cytoplasmic Protein Extraction Kit and pyrrolidine dithiocarbamate (PDTC) were purchased from Beyotime Biotechnology (Haimen, China). Thapsigargin (Tg, T9033) was purchased from Sigma. UltraSYBR Mixture (CW2601M) was purchased from CWBIO biotech Co., Ltd. The antibodies used in this article were as follows: anti-NF-κB p65 (#8242P), anti-phospho-NF-κB p65 (Ser 536, #3033P), anti-IκBα (#4814P) and anti-phospho-IκBα (Ser 32, #2859P) were purchased from Cell Signaling Technology (Beverly, MA, USA). Anti-β-actin (sc-47778), anti-p53 (sc-6243) and anti-PARP (sc-7150) were purchased from Santa Cruz Biotechnology (Santa Cruz, CA, USA). Anti-tubulin (AT819-1) and anti-p21 (AP021) were purchased from Beyotime Biotechnology (Shanghai, China). All primers were synthesized by Sangon Biotech Co. Ltd. (Shanghai, China).

2.2. Cell culture and drug treatments

Papillary thyroid carcinoma BCPAP cells were cultured with RPMI 1640 medium containing 10% newborn calf serum, 100 U/mL penicillin and 100 U/mL streptomycin in a humid atmosphere of 5% (v/v) CO_2 and 95% (v/v) air at 37 °C. Punicalagin was dissolved in methanol to a concentration of 50 mM and stored at −20 °C. Unless otherwise specified, BCPAP cells were treated with 25–100 μM of punicalagin for 24 h [13]. Solvent control contains equal amount of methanol to that of 100 μM of punicalagin. Thapsigargin and PDTC were dissolved in DMSO to a concentration of 1 mM and 100 mM, respectively. These stock solutions were stored at −20 °C until diluted before use.

2.3. MTT assay

BCPAP cells were seeded in a 96-well plate and incubated overnight. After punicalagin treatment, the cells in each well were incubated with 40 μl of MTT (2 mg/ml) at 37 °C for 4 h. Cell supernatants were removed and 100 μl of DMSO per well was added to dissolve the formazan. The absorbance at 490 nm of each well was measured by a microplate reader (μQuant). Cell viability was expressed as a percentage of MTT reduction, assuming that the absorbance of untreated cells was 100%.

2.4. Senescence associated β-Galactosidase (SA-β-gal) staining

Senescence associated β-Galactosidase staining was performed according to the manufacture's protocol (Beyotime Biotechnology, Haimen, China). Briefly, the cells were treated with punicalagin for 24 h and incubated for another 4 days. Then the cells were washed by PBS and fixed for 15 min at room temperature. Subsequently, the cells were washed with PBS for three times and then incubated with 1 ml staining solutions at 37 °C overnight. After that, SA-β-gal staining was observed by a microscope and positive cells in each well were counted in five different fields. All counting results were normalized to that of solvent control group.

2.5. Cell granularity analysis

Cells treated with punicalagin for 24 h were collected and washed twice with PBS. Then the cells were subjected to flow cytometry analysis. Forward scatter (FSC) is directly proportional to cell size and side scatter (SSC) is proportional to cellular granularity. The results were quantified by Cell Quest software.

2.6. Western blot

After drug treatment, the cells were harvested and washed by ice-cold PBS. Next, ice-cold cell lysis (150 mM NaCl, 50 mM Tris-HCl, pH 7.5, 2 mM ethylene diamine tetraacetic acid (EDTA), 1% (w/v) Nonidet P-40, 0.02% (w/v) sodium azide) which contains 1% protease inhibitors (phenylmethylsulfonyl fluoride, PMSF) was added to the cell precipitates. The lysate was subjected to repeated freezing and thawing for three times, and then centrifuged at 12, 000 rpm for 15 min at 4 °C. The supernatant was collected and protein concentration was determined by Bradford assay. Then equivalent amount of proteins were separated by sodium dodecyl sulfate polyacrylamide gel electrophoresis (SDS-PAGE) and were subsequently transferred to a nitrocellulose filter membrane at low temperature. The membrane was blocked by 5% fat-free milk for 1 h and incubated with primary antibody at 4 °C overnight. After being washed by TBST buffer (137 mM NaCl, 20 mM Tris-HCl, 0.1% tween-20, PH 7.6) for three times, the membrane was incubated with corresponding secondary antibody for another 1 h and then washed three times again. The membrane was incubated with ECL chemiluminescence and visualized by film exposure.

2.7. Cell cycle analysis

Cell cycle distribution was determined by PI (Propidium Iodide) staining. The cells were collected after drug treatment and then were fixed by 70% ethanol at 4 °C overnight. Samples were washed by PBS and then incubated with DNA staining reagent containing 0.1% Triton X-100, 0.1 mM EDTA (PH 7.4), 50 μg RNase and 50 μg PI per ml at 37 °C in dark for 30 min. Samples were detected by flow cytometry at FL2-A channel and the data were analyzed by FlowJo software.

2.8. Reverse transcription-polymerase chain reaction (RT-PCR)

After drug treatment, the cells were harvested and total RNA was isolated with TRIzol reagent (Invitrogen, USA) as the manufacturer's directions. First-strand cDNAs were generated by reverse transcription using oligo (dT) from 2 μg of total RNA samples. Following cDNA synthesis, PCR was performed. The condition was shown as followed:

initial denaturation at 95 °C for 5 min, 30 or 35 cycles of denaturation at 95 °C for 30 s, annealing at annealing temperature (Tm) for 30 s, elongation at 72 °C for 30 s, and final extension at 72 °C for 5 min. Most of the PCR products were separated by 1.5% agarose gel electrophoresis (AGE). For *XBP1* splicing detection, the PCR products were separated by 3.5% AGE and visualized by ethidium bromide (20 μg/mL) staining. The sequences of primers used in this article were as follows: *XBP-1*, Forward: 5′-CCTTGTAGTTGAGAACCAGG-3′; Reverse: 5′-GGGGCTTGG TATATATGTGG-3′; *IL-6*, Forward: 5′-GTCCAGTTGCCTTCTCCC-3′, Reverse: 5′-GCCTCTTTGCTGCTTTCA-3′; *IL-1β*, Forward: 5′-ACAGTGG CAATGAGGATG-3′, Reverse: 5′-TGTAGTGGTGGTCGGAGA-3′; *IL-8*, Forward: 5′-ATGACTTCCAAGCTGGCCGTG-3′, Reverse: 5′-TGTGTTGG CGCAGTGTGGTC-3′; *Actin*, Forward: 5′-GCCGGGACCTGACTGAC TAC-3′, Reverse: 5′-CGGATGTCCACGTCACACTT-3′.

2.9. Quantitative real-time polymerase chain reaction (qPCR)

After drug treatment, the RNA was extracted and then reversed as described in 2.8. The obtained cDNA was diluted 5 times and then mixed with 10 μl UltraSYBR Mixture, 4 μl RNase free water, 0.5 μl forward and 0.5 μl reverse primers to a final 20 μl reaction system. PCR was performed with the following conditions: initial denaturation at 95 °C for 5 min, 40 cycles of denaturation at 95 °C for 15 s and annealing at 60 °C for 1 min. The mRNA relative expression level was analyzed by ΔCt method. The sequence of primers used in this article were as follows: *IL-6*, Forward: 5′-TTCTGCGCAGCTTTAAGGAG-3′, Reverse: 5′-AGGTGCCCATGCTACATTTG-3′; *IL-1β*, Forward: 5′- ACAG TGGCAATGAGGATG-3′, Reverse: 5′-TGTAGTGGTGGTCGGAGA-3′; *Actin*, Forward: 5′-GACTTAGTTGCGTTACACCCTTTCT-3′, Reverse: 5′-GCTGTCACCTTCACCGTTCC-3′.

2.10. Statistical analysis

All the data were presented as means ± S.D. of three independent experiments. Statistical significance was determined by one-way ANOVA and *t*-test was used for two groups comparison at equal variance. *$P < 0.05$, represents significant difference, **$P < 0.01$, represents highly significant difference, ***$P < 0.001$, represents extremely significant difference.

3. Results

3.1. Punicalagin induces senescence of BCPAP cells

As is known, all senescent cells display common features, such as larger cell size, granularity, and increased activity of senescence-associated-β-glactosidase (SA-β-gal) [16]. First, the morphological changes of BCPAP cells before and after punicalagin treatment were observed. Compared with solvent control group, punicalagin-treated cells exhibited enlarged and flattened morphology, which is more evident in the group treated with 100 μM of punicalagin (Fig. 1A). The mean value of the cellular area in each group was measured and it showed that cellular area of BCPAP cells significantly elevated in a dose-dependent manner by punicalagin treatment (Fig. 1A). Next, cell granularity was detected by flow cytometry. As expected, cell granularity significantly increased after 25 to 100 μM of punicalagin treatment (Fig. 1B). Furthermore, SA-β-Gal staining assay was performed. As shown in Fig. 1C, punicalagin treatment dose-dependently increased the percent of SA-β-Gal staining positive cells. Compared with solvent control, the rate of SA-β-Gal positive staining cells increased from 3.5 ± 0.7% to 9.5 ± 0.5% and 21.9 ± 6.5% at 50 and 100 μM of punicalagin treatment respectively. Consistent with above observations, SA-β-gal staining positive cells exhibited enlarged cell size and flattened shape. These results suggested punicalagin could induce cellular senescence of BCPAP cells.

3.2. Punicalagin regulates cyclin-dependent kinase inhibitors and causes cell cycle arrest

Halting cell cycle progression is a distinctive feature of senescent cells, which leads to a relatively slow cell growth rate [17]. Our previous studies [13] showed that the cell cycle distribution was merely altered by 100 μM of punicalagin incubation for 24 h. However, a longer duration of incubation, which extended to 72 h, caused a cell cycle arrest at G0/G1 phase (Fig. 2A and B). P53, a well-known tumor suppressor, is also a key mediator of cellular senescence [18]. P53 can integrate many cellular stress signals including DNA damage. When DNA damage is irreparable, phosphorylated p53 promotes senescence *via* transactivation of CDKN1A, which encodes the cyclin dependent kinase inhibitor p21 [19]. The hypo-phosphorylated Rb which is activated by p21 inhibits the transcription of E2F target genes and arrests cells in the cell cycle [20]. As shown in Fig. 2C, punicalagin exposure in a short time failed to alter the protein levels of p53 and p21. Whereas, punicalagin treatment for 72 h augmented the protein expressions of both p53 and p21, which coincided with the cell cycle arrest results mentioned above. Thus, punicalagin-induced cellular senescence of BCPAP cells was confirmed by cell cycle arrest.

3.3. Punicalagin generates SASP in BCPAP cells

It has been verified that cellular senescence is accompanied by altered metabolic activity manifested by an increase in the level of many secreted factors involved in intercellular signaling, such as inflammatory cytokines (*e.g.* IL-1, IL-6) and chemokines (*e.g.* IL-8) [21]. These phenomena are termed as senescence-associated secretory phenotypes (SASP) [22,23]. To further validate the induction of senescence in BCPAP cells by punicalagin, the mRNA levels of *IL-6*, *IL-8* and *IL-1β* were analyzed by RT-PCR. As shown in Fig. 3A, punicalagin dose-dependently enhanced the mRNA expression of *IL-6* and *IL-1β* without affecting *IL-8*. Similar results were obtained from qPCR assay (Fig. 3B). A growing body of evidence suggests that ER stress can also contribute to inflammatory responses [24], which serves as an important regulator of inflammatory genes such as vascular endothelial growth factor (VEGF) and IL-8 [25]. Thapsigargin (Tg), a classic ER stress inducer, significantly increased the mRNA levels of *IL-6, IL-1β* and *IL-8* in BCPAP cells (Fig. 3A). The different expression pattern of inflammatory factors evoked by punicalagin and Tg treatment promoted us to further investigate the effects of punicalagin on the induction of ER stress. Indeed, punicalagin failed to trigger ER stress in BCPAP cells as evidenced by the undetectable X-box binding protein 1 (*XBP1*) mRNA splicing (Fig. 3C), which is a marker of ER stress [26]. Collectively, punicalagin induced senescence and generated SASP in BCPAP cells.

3.4. Punicalagin-induced senescence is mediated by NF-κB activation in BCPAP cells

It has been reported that NF-κB signaling pathway is involved in SASP generation to facilitate senescence [27]. The NF-κB transcription complex consists of two proteins designated p50 and p65. The p50:p65 complex, which is trapped by IκB, retained in the cytoplasm in an inactive form [28]. Upon appropriate activation, IκBα will be phosphorylated, ubiquitinated and eventually degraded, thereby resulting in the release of free NF-κB [29]. The released p65 then translocates to nucleus to activate the transcription of downstream genes [30]. As shown in Fig. 4A, the phosphorylated-IκBα (p-IκBα) was elevated accompanied by a decrease in total IκBα protein as detected by western blot analysis. These results indicated that the phosphorylation and degradation of IκB-α occurred after punicalagin treatment. As expected, punicalagin promoted the phosphorylation of NF-κB/p65 in a dose-dependent manner (Fig. 4B). The subsequent translocation of NF-κB p65 subunit to the nucleus was evaluated by cytoplasm and nuclear cell fraction assay. As shown in Fig. 4C, after 100 μM of punicalagin
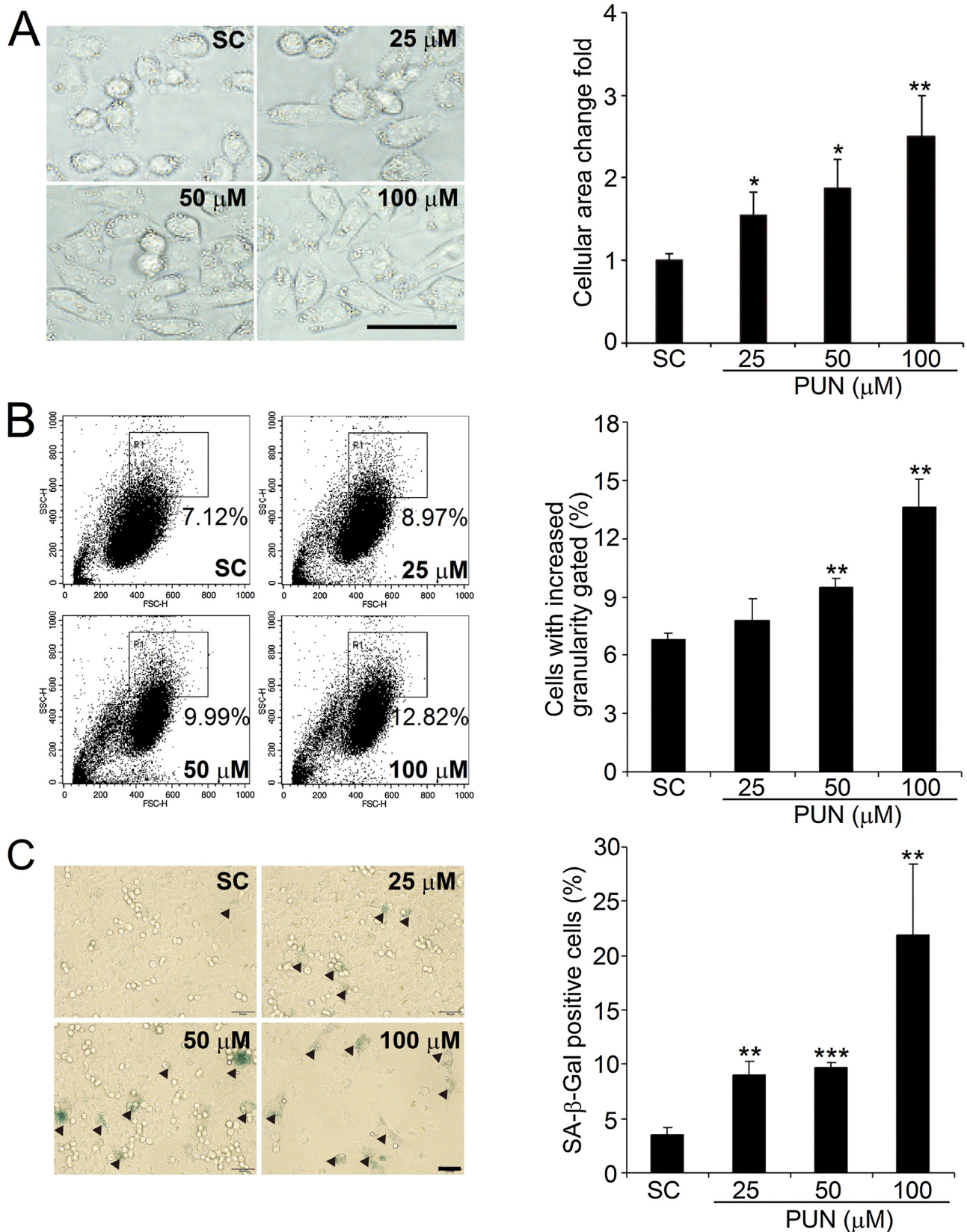
Fig. 1. Punicalagin induces senescence of BCPAP cells. (A) After BCPAP cells were treated with different dosages of punicalagin for 24 h, cell morphology was captured. Scale bar, 20 μm. The area of cell was measured. The average area of 100 cells randomly chosen from 5 fields in each well was calculated. Each value stands for means ± S.D. of three independent experiments (n = 3). *P < 0.05, **P < 0.01 vs. SC group. SC, solvent control. (B) BCPAP cells were treated with punicalagin for 24 h and then cell granularity was analyzed by flow cytometry. The data in histogram were presented as means ± S.D. of three independent experiments (n = 3). **P < 0.01 vs. SC group. (C) BCPAP cells were treated with punicalagin for 24 h. After the withdrawal of the drug, the cells were cultured for additional 4 days. Then the cells were stained for SA-β-gal and observed under a microscope. SA-β-gal staining positive cells appeared green. Scale bar, 20 μm. SA-β-gal positive cells were counted at 3 different fields in each group and the data of histogram were representative of means ± S.D. of three independent experiments (n = 3). **P < 0.01, ***P < 0.001 vs. solvent control.
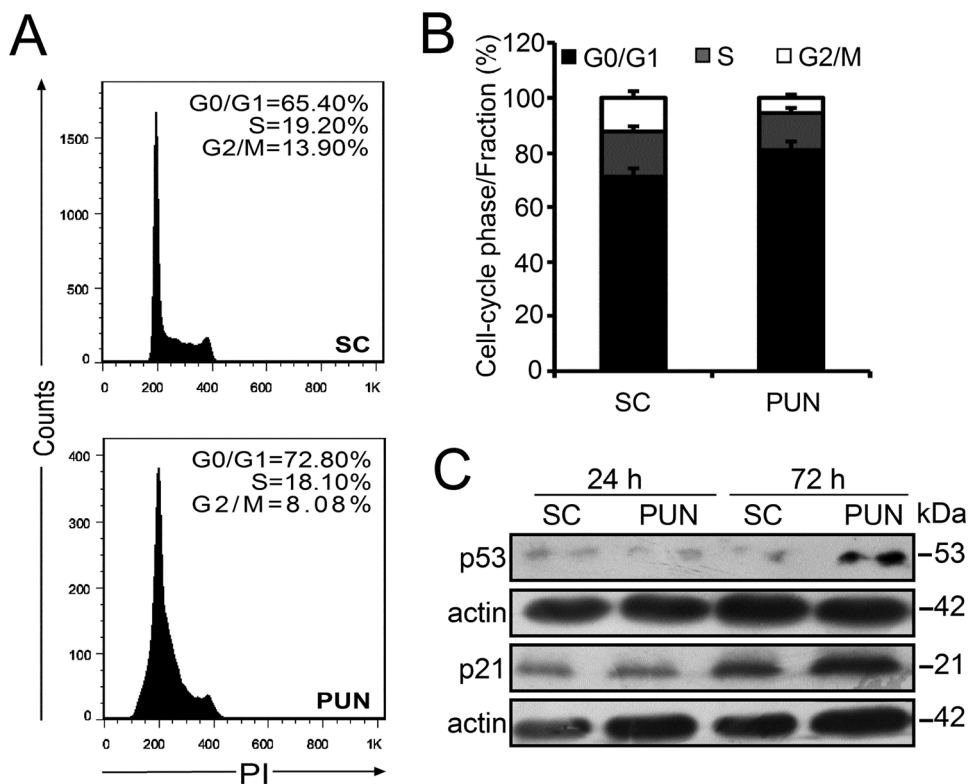
Fig. 2. Punicalagin regulates cyclin-dependent kinase inhibitors and causes cell cycle arrest. (A) BCPAP cells were treated with 100 μM of punicalagin for 72 h. Cells were stained with PI followed by the analysis of cell cycle distribution using flow cytometry. (B) The cell cycle phase distribution was quantified. Histogram was presented as means ± S.D. of three independent experiments (n = 3). (C) BCPAP cells were treated with 100 μM of punicalagin for 72 h. Protein levels of p53 and p21were detected by western blot. β-actin was used as a loading control.

treatment, a portion of p65 translocated from the cytoplasm to the nucleus. The conditional medium collected from punicalagin-treated BCPAP cells was able to trigger the phosphorylation of p65 in thyroid cancer cells as well (Fig. 4D). Moreover, punicalagin-induced phosphorylation of p65 (Fig. 4E) as well as its nuclear translocation (Fig. 4F) was blocked by PDTC, a potent NF-κB inhibitor.

To further confirm the participation of NF-κB signaling in punicalagin-induced senescence, we next examined the changes of senescent features in the presence of PDTC. As shown in Fig. 5A, co-treatment with PDTC markedly reversed the increased SA-β-gal positive staining cells by punicalagin treatment. Compared to punicalagin-treated alone group which had a positive SA-β-gal staining rate at 5.2 ± 1.0%, the combination treatment group showed a higher SA-β-gal staining rate at 15.6 ± 3.6%. In accordance, the induction of SASP was also

ameliorated upon the treatment of PDTC as expected. Compared with control group, punicalagin treatment led to 4.8- and 1.9- fold increase in the mRNA expressions of *IL-6* and *IL-1β* respectively. PDTC markedly reversed punicalagin-induced SASP expression (Fig. 5B). Similar results were obtained by qPCR assay. Upon punicalagin treatment, the mRNA levels *IL-6* and *IL-1β* increased to 2.4 ± 0.85 and 3.0 ± 0.48 fold of that in control group. PDTC decreased the expression folds of *IL-6* and *IL-1β* to 0.91 ± 0.21 and 1.49 ± 0.44 (Fig. 5C). Moreover, PDTC reversed the G0/G1 cell cycle arrest which was induced by punicalagin treatment (Fig. 5D). All these data convincingly showed that punicalagin induced cellular senescent cell cycle arrest in BCPAP cells through the activation of NF-κB signaling pathway.
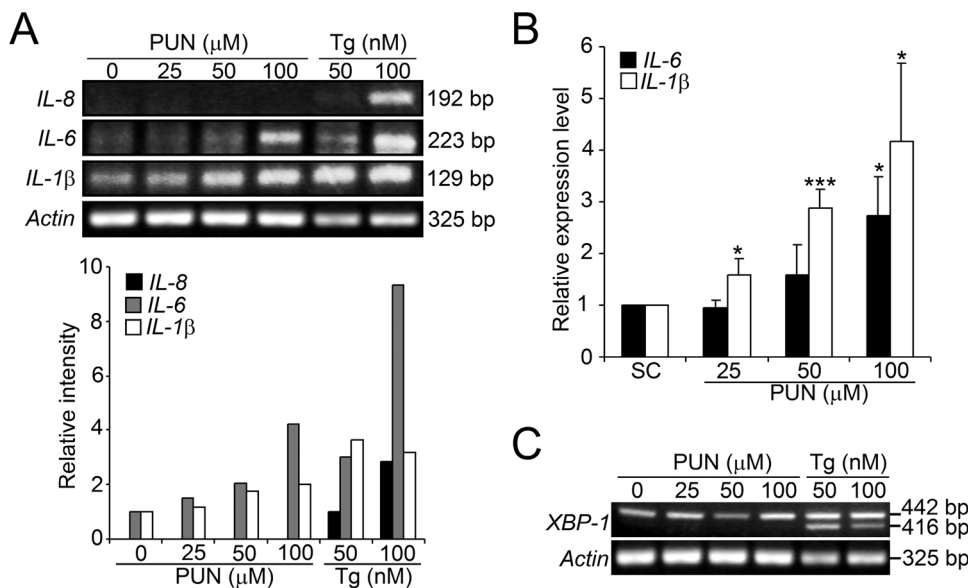

Fig. 3. Punicalagin generates SASP in BCPAP cells. (A) BCPAP cells were treated with punicalagin or thapsigargin for 24 h and then the mRNA levels of *IL-6, IL-1β* and *IL-8* were detected by RT-PCR. *Actin* was used as an internal control. Histogram represented the relative intensity of the corresponding bands. (B) The cells treated with different dosages of punicalagin for 24 h were collected. *IL-6* and *IL-1β* mRNA levels were determined by qPCR and normalized to that of *Actin*. *P < 0.05, ***P < 0.001 *vs.* SC group. SC, solvent control. (C) BCPAP cells were treated as in (A) and then *XBP-1* splicing was detected by RT-PCR.
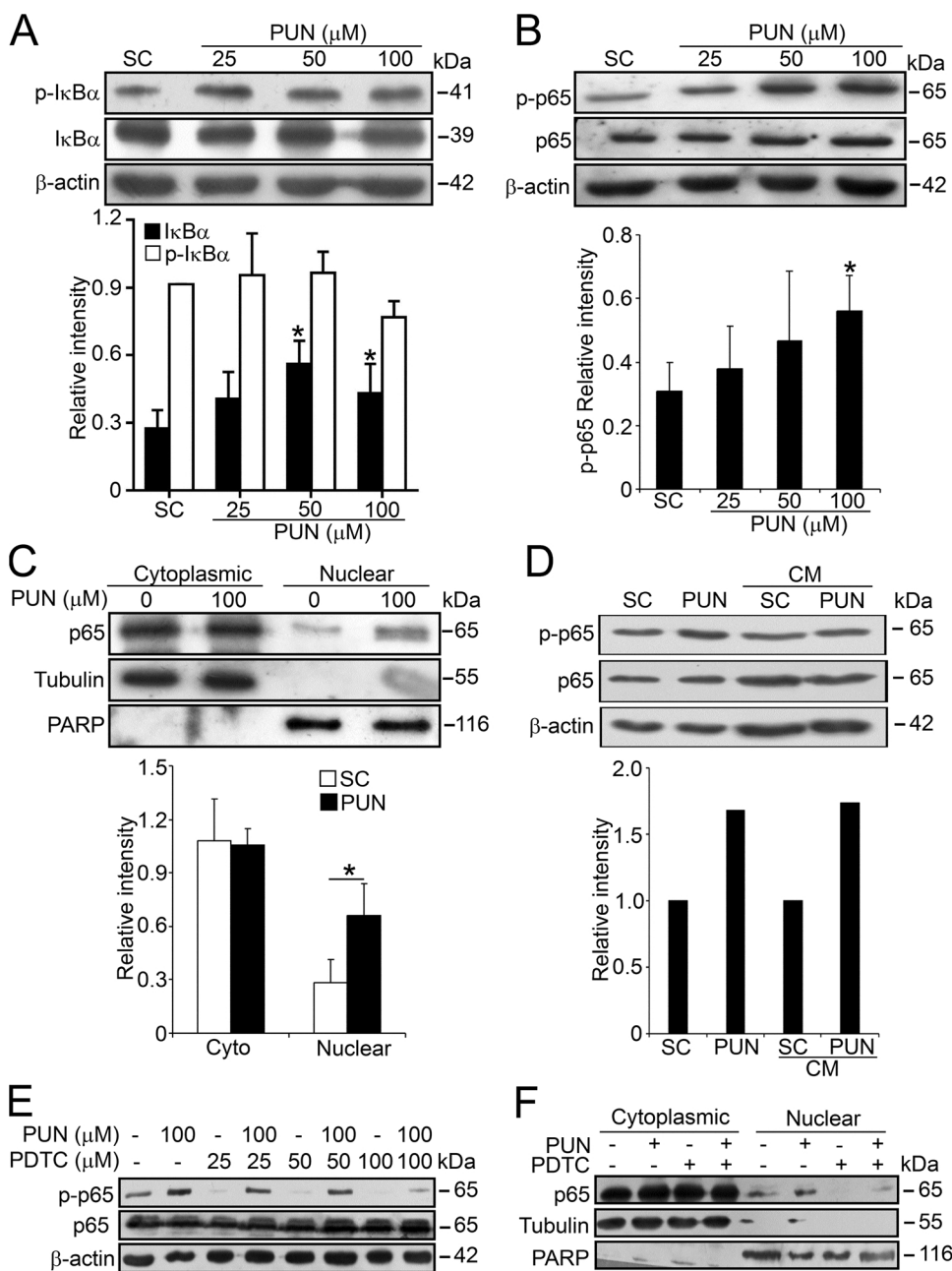
Fig. 4. Punicalagin activates NF-κB signaling in BCPAP cells. (A and B) BCPAP cells were treated with different concentrations of punicalagin (25–100 μM) for 24 h and then the protein levels of IκBα and phosphorylated-IκBα (p-IκBα) were detected by western blot in (A). Phosphorylated (p-p65) and non-phosphorylated p65 (p65) were detected in (B). β-actin was used as a loading control. *$P < 0.05$ vs. SC. SC, solvent control. (C) BCPAP cells were incubated with or without 100 μM of punicalagin for 24 h followed by extraction of cytoplasmic and nuclear fractions. The protein levels of p65 in the cytoplasmic and nuclear fractions were detected by western blot. Tubulin and PARP were used as quality controls for the cytoplasmic and nuclear fractions respectively. Quantified results were shown in histogram and the data stand for means ± S.D. of three independent experiments (n = 3). *$P < 0.05$ vs. solvent control. (D) BCPAP cells were treated with 100 μM punicalagin for 24 h, and then were incubated with fresh medium for another 24 h. The supernatant were collected as conditional medium (CM) and the new seeded BCPAP cells were incubated with CM for another 24 h. Protein levels of p-p65 and p65 were detected by western blot. β-actin was used as a loading control. Quantified results were determined using ImageJ software. (E) BCPAP cells were treated with 100 μM of punicalagin in the presence or absence of different doses of PDTC for 24 h. Protein levels of p-p65 and p65 were detected by western blot. β-actin was used as a loading control. (F) BCPAP cells were incubated with 100 μM of punicalagin in the presence or absence of 100 μM of PDTC for 24 h. The protein levels of p65 in the cytoplasmic and nuclear fractions were detected by western blot.

4. Discussion

Differentiated thyroid cancer (DTC), including papillary, follicular and Hurthle cell subtypes accounts for nearly 93% of all thyroid cancers [31]. Applying surgery, radioactive iodine ablation for remnant thyroid tissue and subsequent TSH suppression are conventional therapy methods for DTC therapy [32]. For patients with distant metastasis after resection of primary DTC, serial treatment of radioactive iodine (RAI) will be applied. If failed to response to RAI therapy, those patients which termed as RAI-refractory DTC (RAI-R-DTC) have to rely on the use of oral kinase inhibitors such as sorafenib, levatinib, sunitinib and vandetanib [33]. Thus, searching for new drugs for DTC treatment remained to be further addressed. Studies by our group and others demonstrated that punicalagin possessed antioxidant, antiinflammatory, antiviral, anti-proliferation and anticancer properties [13]. In the present study, we further illustrated that punicalagin could induce senescent growth inhibition of thyroid cancer cells.

Senescence can be broadly classified into two types, ageing and cellular senescence. Ageing is a reproductive senescence which is a consequence of finite proliferation ability termed as "Hayflick limit" [34]. Cellular senescence is an accelerated permanent cell growth arrest in response to a variety of stimuli like ectopically expression of oncogenes (oncogene-induced senescence, OIS) and chemotherapeutic drugs (therapy-induced senescence, TIS). Both cellular senescence and ageing are closely related to DNA damage responses (DDR). In mammals, DNA damage and mutations accumulate with age. Anti-cancer agents such as adrimycin, cisplatin and multi-kinase inhibitors, which are major TIS inducers, will cause cellular senescence accompanied by DDR [35]. Our previous studies showed that punicalagin triggered DNA damage in an ATM-dependent manner in thyroid cancer cells [14]. It prompted us to speculate that punicalagin might induce tumor cell senescence. In fact, punicalagin induced a senescence-like phenotype with enlarged cell size, flattened cell shape and a terminal cell cycle arrest in papillary thyroid cancer BCPAP cells (Figs. 1 and 2).

NF-κB is a central mediator of the cellular response to diverse insults such as DDR, inflammation and ROS [36]. NF-κB binds to the chromatin
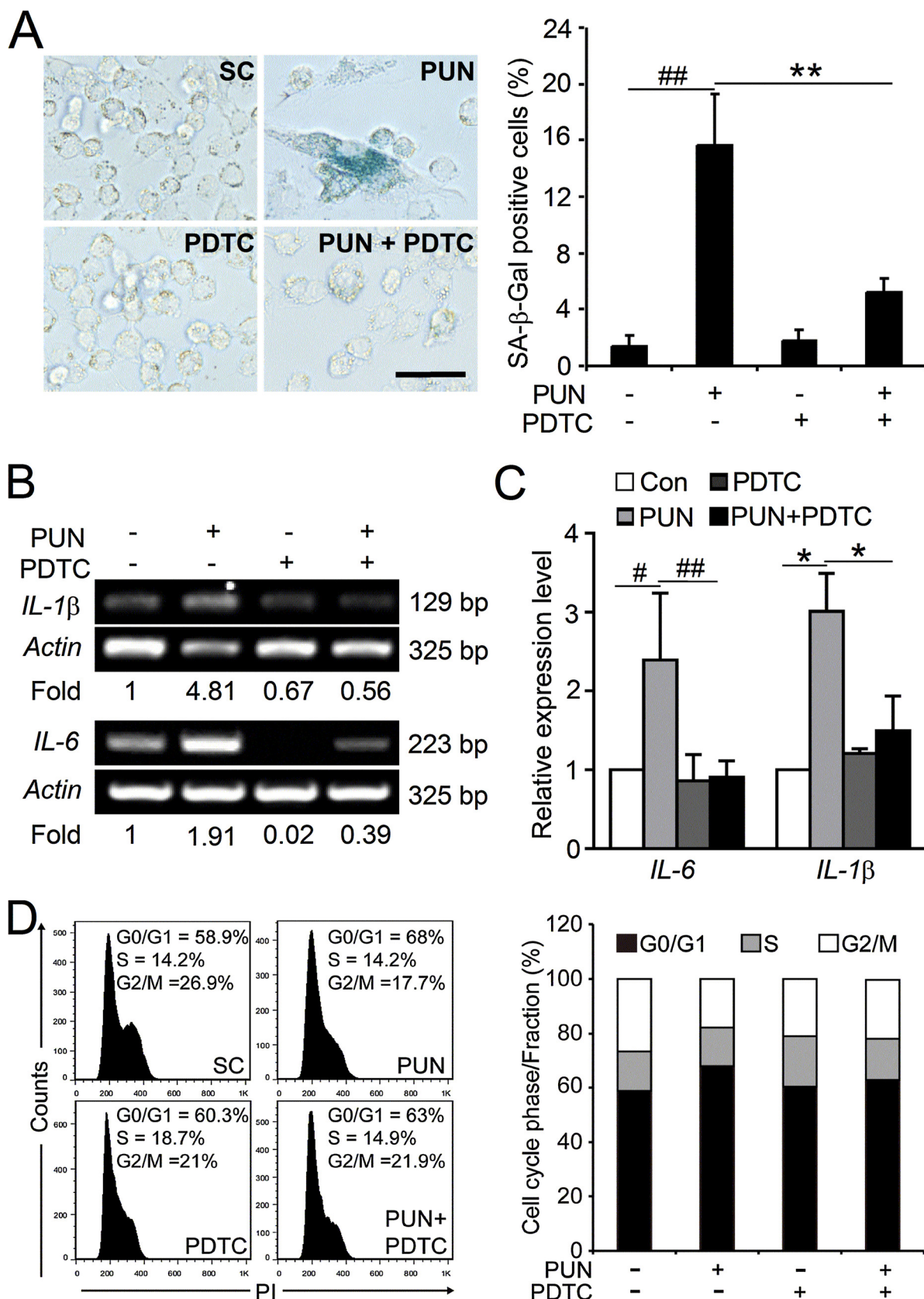
Fig. 5. Punicalagin-induced cellular senescence is reversed by PDTC in BCPAP cells. (A) BCPAP cells were treated with 100 μM of punicalagin in the presence or absence of 100 μM of PDTC for 24 h. After the withdrawal of the drug, the drugs were cultured for additional 4 days. SA-β-gal staining assay was performed and typical micrographs were shown. Scale bar, 20 μm. The percent of SA-β-gal staining positive cells was quantitatively analyzed. $^{\#\#}P < 0.01$, $^{**}P < 0.01$. (B) The mRNA levels of *IL-6* and *IL-1β* were detected by RT-PCR. *Actin* was used as an internal control. The relative expression fold was listed below the corresponding bands. (C) The qPCR analysis of the mRNA levels of *IL-6* and *IL-1β*. $^{\#}P < 0.05$, $^{\#\#}P < 0.01$ *vs.* untreated group, $^{*}P < 0.05$ *vs.* punicalagin-treated alone group. (D) BCPAP cells were treated with 100 μM punicalagin and 100 μM PDTC for 24 h. Cells were stained with PI followed by flow cytometry. The cell cycle distribution was analyzed using Flowjo software (left) and the cell cycle phase distribution was quantified (right).

of senescent cells in a major form of heterodimer of p65 and p50 [37]. Furthermore, NF-κB will induce the secretion of SASP which create a proliferative barrier for cancer cells [38,39]. As shown in our results, cell cycle regulator p53/p21 were activated by punicalagin, resulting in an everlasting cell cycle arrest (Fig. 2). It is our limitation that we have not directly determine the upstream of NF-κB under the treatment of punicalagin. However, numerous reports provoked that DNA damage kinase protein ATM will enhance the signaling of NF-κB. ATM would directly bind to and induce IKKs in cytoplasm through the co-translocation with desumoylated NEMO [36]. Moreover, ATM can also activate IKKs through ATM/TRAF6/cIAP1 signaling [40]. All these findings demonstrated that DNA damage response is closely related to the NF-κB activation. In addition to DDR, ROS production, oxidative phosphorylation and ATP generation also play a central role in cellular senescence [41]. In our previous work, punicalagin was proven to exert its anti-cancer property against thyroid cancer BCPAP cells in a ROS-independent manner [42]. Therefore, we can speculate that the NF-κB mediated senescence which is triggered by punicalagin treatment may majorly depend on DDR in BCPAP cells.

Therapy-induced senescence (TIS) is usually accompanied by senescence-associated secretory phenotype (SASP) secretion including inflammatory cytokines and chemokines [43]. SASP can function in both an autocrine and paracrine modes [43]. On the one hand, SASP reinforces the senescent state of cancer cells, and on the other hand, it induces senescence in the neighboring cells [43]. Consistently, our results showed that punicalagin promoted the induction of SASP which included secreted factors such as IL-6 and IL-1β (Fig. 3). The expressions of these pro-inflammatory factors were mediated by NF-κB activation (Figs. 4 and 5). Whether TIS constitutes a barrier for tumorigenesis or contributes to tumor malignancy remain controversial. It seemed that the efficiency of eliminating the senescent cells by recruiting tumor-infiltrating immune cells decided the destiny of senescence into tumor inhibition or progression [43]. Of note, certain inspiring works demonstrated that targeting senescence will be a promising method for cancer therapy. It has been verified that induction of senescence in mice delayed cancer recurrence and markedly rescued the poor prognosis [44]. In another case, the combination of senescence induction with BRAF inhibition dramatically inhibited the melanoma tumorigenesis and sensitized the cancer cells to the treatment of PLX4770, a BRAF inhibitor [45]. Collectively, senescence is a potential target for cancer therapy.

Punicalagin is a large polyphenol compound and belongs to a family of ellagitannins which can be further hydrolyzed [46]. The released ellagic acid entered circulation in a prolonged manner [47]. In prostate cancer clinical trials, 370 mg/day oral consumption of punicalagin provides a significant prolongation of PSA doubling time without severe adverse effects [48]. Comparably, 100 μM of punicalagin which equals to 25 mg/250 ml in human beings is reachable in clinic and have a good response of senescence in thyroid cancer cells. Though more well-designed clinical trials are needed to pave, our research suggests a new therapeutic prospect for malignant thyroid cancer treatment.

5. Conclusions

In the present study, we further uncovered the anti-cancer mechanism of punicalagin against thyroid cancer. After a quick elimination by autophagic cell death which was triggered by punicalagin treatment within 24 h [13], the remnant cancer cells underwent a growth arrest in an accelerated senescent manner. Our work not only highlighted the potential value of punicalagin in thyroid cancer treatment but also provided a novel view of targeting senescence for thyroid cancer therapy.

Acknowledgements

References

[1] I.B. Roninon, Tumor cell senescence in cancer treatment, Cancer Res. 63 (2003) 2705–2715 doi: published June 2003.

[2] A. Lauri, G. Pompilio, M.C. Capogrossi, The mitochondrial genome in aging and senescence, Ageing Res. Rev. 18 (2014) 1–15, http://dx.doi.org/10.1016/j.arr. 2014.07.001.

[3] M. Collado, M. Serrano, Senescence in tumours: evidence from mice and humans, Nat. Rev. Cancer. 10 (2010) 51–57, http://dx.doi.org/10.1038/nrc2772.

[4] J.P. Coppe, P.Y. Desprez, A. Krtolica, J. Campisi, The senescence-associated secretory phenotype: the dark side of tumor suppression, Annu. Rev. Pathol. 5 (2010) 99–118, http://dx.doi.org/10.1146/annurev-pathol-121808-102144.

[5] A.W. Shao, et al., Bclaf1 is an important NF-kappaB signaling transducer and C/EBPbeta regulator in DNA damage-induced senescence, Cell Death Differ. 23 (2016) 865–875, http://dx.doi.org/10.1038/cdd.2015.150.

[6] W. Xue, et al., Senescence and tumour clearance is triggered by p53 restoration in murine liver carcinomas, Nature. 445 (2007) 656–660, http://dx.doi.org/10.1038/nature05529.

[7] A. Alimonti, et al., A novel type of cellular senescence that can be enhanced in mouse models and human tumor xenografts to suppress prostate tumorigenesis, J. Clin. Invest. 120 (2010) 681–693, http://dx.doi.org/10.1172/JCI40535.

[8] T.S. Nowicki, et al., Downregulation of uPAR inhibits migration, invasion, proliferation, FAK/PI3K/Akt signaling and induces senescence in papillary thyroid carcinoma cells, Cell Cycle 10 (1) (2011) 100–107, http://dx.doi.org/10.4161/cc. 10.1.14362.

[9] R.L. Siegel, K.D. Miller, A. Jemal, Cancer statistics, 2017, CA Cancer J. Clin. 67 (2017) 7–30, http://dx.doi.org/10.3322/caac.21387.

[10] C. Papewalis, M. Ehlers, M. Schott, Advances in cellular therapy for the treatment of thyroid cancer, J. Oncol. 2010 (2010) 179491, http://dx.doi.org/10.1155/2010/179491.

[11] K.T. Yeung, E.E. Cohen, Lenvatinib in advanced, radioactive iodine-refractory, differentiated thyroid carcinoma, Clin. Cancer Res. 21 (2015) 5420–5426, http://dx.doi.org/10.1158/1078-0432.ccr-15-0923.

[12] S.G. Wang, et al., Punicalagin induces apoptotic and autophagic cell death in human U87MG glioma cells, Acta Pharmacol. Sin. 34 (2013) 1411–1419, http://dx.doi.org/10.1038/aps.2013.98.

[13] X. Cheng, et al., Punicalagin induces apoptosis-independent autophagic cell death in human papillary thyroid carcinoma BCPAP cells, RSC Adv. 6 (72) (2016) 68485–68493, http://dx.doi.org/10.1039/c6ra13431a.

[14] X. Yao, et al., Punicalagin from pomegranate promotes human papillary thyroid carcinoma BCPAP cell death by triggering ATM-mediated DNA damage response, Nutr. Res. 47 (2017) 63–71, http://dx.doi.org/10.1016/j.nutres.2017.09.001.

[15] E.C. Filippi-Chiela, M.M. Bueno e Silva, M.P. Thome, G. Lenz, Single-cell analysis challenges the connection between autophagy and senescence induced by DNA damage, Autophagy 11 (2015) 1099–1113, http://dx.doi.org/10.1080/15548627. 2015.1009795.

[16] E. Sikora, T. Arendt, M. Bennett, M. Narita, Impact of cellular senescence signature on ageing research, Ageing Res. Rev. 10 (2011) 146–152, http://dx.doi.org/10. 1016/j.arr.2010.10.002.

[17] F. Rodier, J. Campisi, Four faces of cellular senescence, J. Cell Biol. 192 (2011) 547–556, http://dx.doi.org/10.1083/jcb.201009094.

[18] Y. Qian, X. Chen, Tumor suppression by p53: making cells senescent, Histol. Histopathol. 25 (2010) 515–526, http://dx.doi.org/10.14670/HH-25.515.

[19] F. d'Adda di Fagagna, Living on a break: cellular senescence as a DNA-damage response, Nat. Rev. Cancer 8 (2008) 512–522, http://dx.doi.org/10.1038/nrc2440.

[20] J. Campisi, Cellular senescence as a tumor-suppressor mechanism, Trends Cell Biol. 11 (2001) S27–31, http://dx.doi.org/10.1016/S0962-8924(01)02151-1.

[21] A.R. Davalos, J.P. Coppe, J. Campisi, P.Y. Desprez, Senescent cells as a source of inflammatory factors for tumor progression, Cancer Metastasis Rev. 29 (2010) 273–283, http://dx.doi.org/10.1007/s10555-010-9220-9.

[22] C. Kang, et al., The DNA damage response induces inflammation and senescence by inhibiting autophagy of GATA4, Science 349 (2015) aaa5612, http://dx.doi.org/10. 1126/science.aaa5612.

[23] H. Chen, P.D. Ruiz, W.M. McKimpson, L. Novikov, R.N. Kitsis, M.J. Gamble, MacroH2A1 and ATM play opposing roles in paracrine senescence and the senescence-Associated secretory phenotype, Mol. Cell 59 (2015) 719–731, http://dx.doi.org/10.1016/j.molcel.2015.07.011.

[24] K. Zhang, R.J. Kaufman, From endoplasmic-reticulum stress to the inflammatory response, Nature 454 (2008) 455–462, http://dx.doi.org/10.1038/nature07203.

[25] P.L. Marjon, E.V. Bobrovnikova-Marjon, S.F. Abcouwer, Expression of the pro-angiogenic factors vascular endothelial growth factor and interleukin-8/CXCL8 by human breast carcinomas is responsive to nutrient deprivation and endoplasmic reticulum stress, Mol. Cancer 3 (4) (2004) http://dx.doi.org/10.1186/1476-4598-3-4.

[26] M. Calfon, et al., IRE1 couples endoplasmic reticulum load to secretory capacity by processing the XBP-1 mRNA, Nature 415 (2002) 92–96, http://dx.doi.org/10.1038/415092a.

[27] H. Guo, et al., Chemokine receptor CXCR2 is transactivated by p53 and induces p38-mediated cellular senescence in response to DNA damage, Aging Cell 12 (2013) 1110–1121, http://dx.doi.org/10.1111/acel.12138.

[28] P.A. Baeuerle, The inducible transcription activator NF-kappa B: regulation by distinct protein subunits, Biochim. Biophys Acta. 1072 (1991) 63–80, http://dx.doi.org/10.1016/0304-419X(91)90007-8.

[29] G. Natoli, S. Chiocca, Nuclear ubiquitin ligases, NF-kappaB degradation, and the control of inflammation, Sci. Signal. 1 (2008), http://dx.doi.org/10.1126/stke.11pe1 pe1.

[30] S. Ghosh, M. Karin, Missing pieces in the NF-kappaB puzzle, Cell 109 (Suppl) (2002) S81–S96, http://dx.doi.org/10.1016/S0092-8674(02)00703-1.

[31] J.J. Gruber, A.D. Colevas, Differentiated thyroid cancer: focus on emerging treatments for radioactive iodine-refractory patients, Oncologist 20 (2015) 113–126, http://dx.doi.org/10.1634/theoncologist.2014-0313.

[32] J.K. Byrd, et al., Well differentiated thyroid carcinoma: current treatment, Curr. Treat. Options Oncol. 13 (2012) 47–57, http://dx.doi.org/10.1007/s11864-011-0173-1.

[33] R.M. Carneiro, et al., Targeted therapies in advanced differentiated thyroid cancer, Cancer Treat. Rev. 41 (2015) 690–698, http://dx.doi.org/10.1016/j.ctrv.2015.06.002.

[34] B.A. Benayoun, E.A. Pollina, A. Brunet, Epigenetic regulation of ageing: linking environmental inputs to genomic stability, Nat. Rev. Mol. Cell Biol. 16 (2015) 593–610, http://dx.doi.org/10.1038/nrm4048.

[35] D.A. Gewirtz, S.E. Holt, L.W. Elmore, Accelerated senescence: an emerging role in tumor cell response to chemotherapy and radiation, Biochem. Pharmacol. 76 (2008) 947–957, http://dx.doi.org/10.1016/j.bcp.2008.06.024.

[36] A. Salminen, A. Kauppinen, K. Kaarniranta, Emerging role of NF-κB signaling in the induction of senescence-associated secretory phenotype (SASP), Cell Signal. 24 (2012) 835–845, http://dx.doi.org/10.1016/j.cellsig.2011.12.006.

[37] Y. Chien, et al., Control of the senescence-associated secretory phenotype by NF- B promotes senescence and enhances chemosensitivity, Genes Dev. 25 (2011) 2125–2136, http://dx.doi.org/10.1101/gad.17276711.

[38] J.S. Tilstra, et al., NF-κB inhibition delays DNA damage–induced senescence and aging in mice, J. Clin. Invest. 122 (2012) 2601–2612, http://dx.doi.org/10.1172/jci45785.

[39] M. Lesina, et al., RelA regulates CXCL1/CXCR2-dependent oncogene-induced senescence in murine Kras-driven pancreatic carcinogenesis, J. Clin. Invest. 126 (2016) 2919–2932, http://dx.doi.org/10.1172/JCI86477.

[40] M. Hinz, et al., A cytoplasmic ATM-TRAF6-cIAP1 module links nuclear DNA damage signaling to ubiquitin-mediated NF-kappaB activation, Mol. Cell 40 (2010) 63–74, http://dx.doi.org/10.1016/j.molcel.2010.09.008.

[41] F. Prattichizzo, et al., Short-term sustained hyperglycaemia fosters an archetypal senescence-associated secretory phenotype in endothelial cells and macrophages, Redox Biol. 15 (2018) 170–181, http://dx.doi.org/10.1016/j.redox.2017.12.001.

[42] X. Yao, et al., Punicalagin from pomegranate promotes human papillary thyroid carcinoma BCPAP cell death by triggering ATM-mediated DNA damage response, Nutr. Res. 47 (2017) 63–71, http://dx.doi.org/10.1016/j.nutres.2017.09.001.

[43] D. Di Mitri, A. Alimonti, Non-Cell-Autonomous regulation of cellular senescence in cancer, Trends Cell Biol. 26 (2016) 215–226, http://dx.doi.org/10.1016/j.tcb.2015.10.005.

[44] C.A. Schmitt, et al., A senescence program controlled by p53 and p16INK4a contributes to the outcome of cancer therapy, Cell 109 (2002) 335–346, http://dx.doi.org/10.1016/S0092-8674(02)00734-1.

[45] J. Kaplon, et al., A key role for mitochondrial gatekeeper pyruvate dehydrogenase in oncogene-induced senescence, Nature. 498 (2013) 109–112, http://dx.doi.org/10.1038/nature12154.

[46] E. Turrini, L. Ferruzzi, C. Fimognari, Potential effects of pomegranate polyphenols in cancer prevention and therapy, Oxid. Med. Cell Longev. 2015 (2015) 938475, http://dx.doi.org/10.1155/2015/938475.

[47] M.A. Nuñez-Sánchez, et al., Targeted metabolic profiling of pomegranate polyphenols and urolithins in plasma, urine and colon tissues from colorectal cancer patients, Mol. Nutr. Food Res. 58 (2014) 1199–1211, http://dx.doi.org/10.1002/mnfr.201300931.

[48] C.J. Paller, et al., A randomized phase II study of pomegranate extract for men with rising PSA following initial therapy for localized prostate cancer, Prostate Cancer Prostatic Dis. 16 (2012) 50–55, http://dx.doi.org/10.1038/pcan.2012.20.